

Purinergic 2X7 Receptor is Involved in the Podocyte Damage of Obesity-Related Glomerulopathy via Activating Nucleotide-Binding and Oligomerization Domain-Like Receptor Protein 3 Inflammasome

Xiao-Xia Hou, Hong-Rui Dong, Li-Jun Sun, Min Yang, Hong Cheng, Yi-Pu Chen

Division of Nephrology, Beijing Anzhen Hospital, Capital Medical University, Beijing 100029, China

Abstract

Background: The nucleotide-binding and oligomerization domain-like receptor protein 3 (NLRP3) inflammasome composed of NLRP3, apoptosis-associated speck-like protein containing CARD (ASC), and caspase-1 is engaged in the inflammatory response of many kidney diseases and can be activated by purinergic 2X7 receptor (P2X7R). This study was conducted to explore whether P2X7R plays a pathogenic role in the podocyte damage of obesity-related glomerulopathy (ORG) and whether this role is mediated by the activation of NLRP3 inflammasome.

Methods: A mouse model of ORG was established by high-fat diet feeding. The conditionally immortalized mouse podocytes were cultured with leptin or with leptin and P2X7R antagonist (KN-62 or A438079). The mRNA and protein expression of the P2X7R and NLRP3 inflammasome components including NLRP3, ASC, and caspase-1, as well as the podocyte-associated molecules including nephrin, podocin, and desmin in mouse renal cortex or cultured mouse podocytes were tested by real-time-polymerase chain reaction and Western blot analysis, respectively.

Results: The significantly upregulated expression of P2X7R and NLRP3 inflammasome components and the NLRP3 inflammasome activation were observed in the renal cortex (in fact their location in podocytes was proved by confocal microscopy) of ORG mice *in vivo*, which were accompanied with the morphological changes of podocyte damage and the expression changes of podocyte-associated molecules. Similar changes in the expression of P2X7R and NLRP3 inflammasome components as well as in the expression of podocyte-associated molecules were also observed in the cultured podocyte studies treated by leptin *in vitro*, and all of the above changes were significantly attenuated by the P2X7R antagonist KN-62 or A438079.

Conclusions: P2X7R could trigger the activation of NLRP3 inflammasome, and the activated P2X7R/NLRP3 inflammasome in podocytes might be involved in the podocyte damage of ORG.

Key words: Desmin; Nucleotide-Binding and Oligomerization Domain-Like Receptor Protein 3 Inflammasome; Obesity-Related Glomerulopathy; Podocytes; Purinergic 2X7 Receptor

INTRODUCTION

At present, obesity is one of the global public health concern crises and its prevalence has more than doubled worldwide over the past few decades.^[1] Data from many studies have shown that obesity is an important and independent risk factor for the occurrence and progression of chronic kidney disease.^[2,3] In 1974, the link between obesity and massive proteinuria was first reported by Weisinger *et al.*^[4] Since then, more and more evidence had demonstrated that obesity could directly induce glomerular

structural and functional changes, namely obesity-related glomerulopathy (ORG).^[3,5] Currently, the rapid growth of

Address for correspondence: Prof. Yi-Pu Chen,
Division of Nephrology, Beijing Anzhen Hospital, Capital Medical
University, Beijing 100029, China
E-Mail: chen_yipu@163.com

This is an open access journal, and articles are distributed under the terms of the Creative Commons Attribution-NonCommercial-ShareAlike 4.0 License, which allows others to remix, tweak, and build upon the work non-commercially, as long as appropriate credit is given and the new creations are licensed under the identical terms.

For reprints contact: reprints@medknow.com

© 2018 Chinese Medical Journal | Produced by Wolters Kluwer - Medknow

Received: 26-09-2018 **Edited by:** Xin Chen

How to cite this article: Hou XX, Dong HR, Sun LJ, Yang M, Cheng H, Chen YP. Purinergic 2X7 Receptor is Involved in the Podocyte Damage of Obesity-Related Glomerulopathy via Activating Nucleotide-Binding and Oligomerization Domain-Like Receptor Protein 3 Inflammasome. *Chin Med J* 2018;131:2713-25.

Access this article online

Quick Response Code:



Website:
www.cmj.org

DOI:
10.4103/0366-6999.245270

obesity across the globe including China contributes to an increased incidence of ORG.^[3,5-7]

Podocytes with their interdigitated foot processes cover the glomerular capillary surface and constitute the major component of the glomerular filtration barrier.^[8,9] The structural and functional disruption of podocytes will lead to proteinuria and renal dysfunction in kidney diseases including ORG.^[10] Many studies on patients with ORG and animal model of ORG have illustrated that the podocyte damage was the hallmark of ORG.^[11,12] Now, it is generally recognized that podocyte damage might play a pivotal role in the occurrence and progression of ORG.^[13]

The mechanism of podocyte damage in ORG has not yet been fully elucidated. In recent years, the pathogenic role of inflammation including nucleotide-binding and oligomerization domain-like receptor protein 3 (NLRP3) inflammasome in ORG has attracted much attention of researchers. NLRP3 inflammasome is an intracellular multiprotein complex and consists of NLRP3, apoptosis-associated speck-like protein containing CARD (ASC, an adaptor protein of the inflammasome), and caspase-1 (cysteine-requiring aspartate protease-1, an effector protein of the inflammasome, which usually exists in the form of inactive pro-caspase-1). After the NLRP3 is acted by an activation signal, activation of the NLRP3 will result in the assembly of the NLRP3/ASC/pro-caspase-1 complex and trigger the autocatalytic cleavage of pro-caspase-1 to form its active p10 and p20 subunits, which are responsible for the processing and secretion of the inflammatory cytokines such as interleukin (IL)-18 and IL-1 β .^[14-16]

NLRP3 inflammasome can be activated by a lot of exogenous and endogenous substances, in which extracellular adenosine triphosphate (eATP) and its receptor, the purinergic 2X7 receptor (P2X7R), are of particular concern. P2X7R, a member of the purinergic receptor family, is a ligand-gated cation channel. eATP binding to P2X7R causes P2X7R activation and rapid opening of cation channel, leading to outflow of potassium ion and depletion of intracellular potassium ion, which are necessary for NLRP3 inflammasome activation.^[17-19]

In 2013, Solini *et al.*^[17] reported that the mRNA and/or protein expression of P2X7R and the components of NLRP3 inflammasome were significantly upregulated in the cultured mouse podocytes stimulated by lipopolysaccharide and 2'(3')-O-(4-benzoylbenzoyl) ATP (BzATP, a potent P2X7R agonist) and in the renal cortex of the mice with metabolic syndrome and elevated blood glucose. All the above changes could be attenuated by the *P2X7R* gene silencing of cultured podocytes and gene knockout of mouse model.^[17] The above findings promoted us to explore the possible pathogenic role of P2X7R and NLRP3 inflammasome in the podocyte damage of ORG.

The research was carried out on the mouse model of ORG induced by high-fat diet (HFD) feeding as well as in the

cultured conditionally immortalized mouse podocytes treated with leptin. The results of these studies *in vivo* and *in vitro* suggested that P2X7R is involved in the podocyte damage of ORG via NLRP3 inflammasome activation.

METHODS

Ethical approval

All animal care and experimental protocols complied with the US National Institutes of Health Guide for the Care and Use of Laboratory Animals (publication no. 85-23, 1996) and were approved by the Institutional Animal Care and Use Committee of Capital Medical University.

Mouse model and grouping

Fourteen male C57BL/6J mice (5 weeks old) were purchased from Huaifukang Bioscience Co., Beijing, China. Before the experiments, an identification of genetic background for the experimental mice was conducted [Supplementary Material 1]. Mice were housed in the animal room at a temperature of 22°C with a relative humidity of 55%. All mice were adaptively fed with a low-fat diet (LFD, Research Diets, D12490B), in which fat accounts for 10% of all calories, for a week before experiments. Then, the mice were randomly divided into control group and model group (seven mice in each group). In the former, the mice continued to be fed with LFD and in the latter, the mice were fed with a HFD (Research Diets, D12492), in which fat accounts for 60% of all calories. All the mice were sacrificed at the end of 12th week. About three-quarters of cortex tissue of the left kidney was fixed in 4% neutral formaldehyde solution for light microscopy, and the remaining cortex tissue of the left kidney was fixed in 2.5% glutaraldehyde solution for electron microscopy. About a quarter of cortex tissue of the right kidney was embedded in optimal cutting temperature compound (Tissue-Tek, Japan), wrapped in aluminum foil, and placed in liquid nitrogen immediately for confocal microscopy, and the remaining cortex tissue of the right kidney was rapidly preserved in liquid nitrogen for real-time-polymerase chain reaction (PCR) and Western blot assays.

Biological parameters

Body weight was measured every week and body length was measured at the end of 12th week. The weight of kidney as well as abdominal fat, perirenal fat, and periepididymal fat was separately measured after the mouse was sacrificed. Then, the following indexes were calculated:^[12] Lee's index = (body weight [g] \times 1000)^{1/3} \div (body length [cm]); abdominal fat index = (abdominal fat mass [g] \div body weight [g]) \times 100%; perirenal fat index = (perirenal fat mass [g] \div body weight [g]) \times 100%; and periepididymal fat index = (periepididymal fat mass [g] \div body weight [g]) \times 100%.

The mice were placed into metabolic cages individually to collect nocturnal 12 h urine sample for the detection of urinary protein excretion at 0 week and at 12th week as well as of urine creatinine at the end of 12th week.

Blood sample of each mouse was collected to test blood glucose, serum cholesterol, serum triglycerides, and serum creatinine at the end of 12th week. Creatinine clearance rate (CCr) was calculated, according to the following formula: $CCr \text{ (ml/min)} = \text{urine creatinine } (\mu\text{mol/L}) \times \text{urine volume (ml/min)} \div \text{serum creatinine } (\mu\text{mol/L})$.^[12]

Renal histological examination

After fixation in 4% neutral formaldehyde solution, the renal cortex tissue was conventionally dehydrated, permeabilized, embedded in paraffin, and then cut into 3- μm thick sections using a microtome (SAKURA Tissue-Tek, Japan). The sections were stained with periodic acid–Schiff reagent. For every mouse, twenty images of glomerular maximal profiles with vascular pole and/or urinary pole were taken under a high-power microscope ($\times 400$, Olympus, Tokyo, Japan) and then were analyzed by the Nikon NIS-Elements BR image analysis software (Nikon, Tokyo, Japan). The two longest perpendicular diameters of every glomerular capillary tuft without Bowman's space were measured and their mean value was calculated.^[12]

In addition, images of twenty random visual fields mainly containing tubules and interstitium were taken under a low-power microscope ($\times 200$) and then analyzed by Nikon NIS-Elements BR image analysis software. The total area of tubules with cytoplasmic vacuolar degeneration and the total area of glomeruli in each visual field were measured. The relative area of tubules with cytoplasmic vacuolar degeneration (%) was calculated with the following formula: $\text{the total area of tubules with cytoplasmic vacuolar degeneration} \div (\text{the area of visual field} - \text{the total area of glomeruli}) \times 100\%$.

Oil red O staining

Frozen kidney tissue was cut into 10- μm thick sections and dried in a fume hood. After washing three times with distilled water, the sections were immersed in 60% isopropyl alcohol for 30 s and then stained with oil red O solution (Urchem, China) (0.5 g oil red O was dissolved in 100 ml isopropyl alcohol as stock solution, and then the stock solution was diluted with distilled water to 60% concentration as working solution) for 20 min. Then, the sections were washed, counterstained with hematoxylin, and mounted for the assessment of renal lipid accumulation.^[17]

Foot process width measurement

After fixation in 1.5% glutaraldehyde and 1% osmium tetroxide, the renal cortex tissue was conventionally dehydrated and embedded in epoxy resin. The semi-thin sections were cut and stained with toluidine blue to locate the nonsclerosed glomeruli. Subsequently, the ultra-thin sections containing one or two glomeruli were made and stained with uranium acetate-lead citrate. For each specimen, ten photographs ($\times 20,000$) covering various regions in the glomerular cross-section were taken under electron microscopy. By using Nikon NIS-Elements BR image analysis software, the length of the peripheral GBM was measured and the number of slit pores overlying this GBM

length was counted. The mean of the foot process width (\overline{W}_{FP}) was calculated using the following formula:

$$\overline{W}_{FP} = \frac{\pi}{4} \times \frac{\sum \text{GBM length}}{\sum \text{slits}}$$

Where $\sum \text{slits}$ is the total number of slits counted and $\sum \text{GBM length}$ is the total GBM length measured in one glomerulus.^[20]

Double-immunofluorescent staining and confocal microscopy

Double-immunofluorescent staining was performed on the sections of frozen mouse kidney tissue. The sections were incubated with rabbit anti-P2X7R antibody (1:200, Alomone, APR-004), rabbit anti-NLRP3 antibody (1:200, NOVUS, NBP-12448), and Guinea pig anti-nephrin antibody (1:200, PROPEN, GP-N2) for overnight at 4°C. After washing, the sections were incubated with Alexa 555 labeled goat anti-rabbit secondary antibody (1:50, Invitrogen, A-32732) and Alexa 488 labeled goat anti-Guinea pig secondary antibody (1:50, Invitrogen, A-11073) for 30 min at 37°C. After washing, the sections were mounted with a mounting solution containing DAPI and then observed with a confocal laser scanning microscope (Leica TSC SP5II, Germany).^[21]

Podocyte culture and grouping

The conditionally immortalized mouse podocyte cell line was provided by Professor Maria Pia Rastaldi (S. Carlo Hospital, University of Milan, Italy) and cultured as described previously.^[12] Well-differentiated immortalized mouse podocytes were used for experiments. The podocytes were incubated with the RPMI-1640 medium with 5% fetal bovine serum and grouped as follows: medium alone; medium containing leptin (Abcam, UK); medium containing A438079 (Tocris Bioscience, UK) or KN-62 (Sigma-Aldrich, USA); and medium containing both leptin and A438079 or leptin and KN-62 (cells were preincubated with A438079 or KN-62 for 30 min, and then leptin was added in the culture medium). The concentrations of leptin, KN-62, and A438079 in the medium were 20 ng/ml, 2.5 $\mu\text{mol/L}$, and 10 $\mu\text{mol/L}$, respectively, of which all had no cytotoxic effects on podocytes confirmed by lactate dehydrogenase (LDH) release assay [Supplementary Material 1].^[21]

Real-time-polymerase chain reaction

Total RNA from renal cortex tissue or cultured podocytes was extracted using the Trizol reagent (Invitrogen, USA) according to the manufacturer's instructions. RNA (2 μg) from each sample was reverse-transcribed to cDNA with EasyScript First-Strand cDNA Synthesis SuperMix (TransGen Biotech, China). Gene-specific primers were designed and synthesized by SBS Genetech Co. (China) [Supplementary Table 1]. Quantitative real-time-PCR was performed according to the procedures described previously.^[12]

Western blot analysis

Total protein from renal cortex tissue or cultured podocytes was extracted using RIPA lysis buffer. The concentration of protein was measured by a BCA protein assay kit (Beyotime

Biotech, China). The extracted protein sample was boiled for 5 min. The proteins in each sample were separated by 10% or 12% sodium dodecyl sulfate-polyacrylamide gel electrophoresis and then transferred to nitrocellulose membrane (GE Healthcare, USA). After blocking with 5% skim milk in phosphate-buffered saline with 0.1% Tween 20 for 1 h, the membrane was incubated with various primary antibodies overnight at 4°C and then with the corresponding secondary antibody at room temperature for 1 h [all the primary and secondary antibodies are listed in Supplementary Table 2]. Finally, the blotted protein in each strip was semi-quantified using an Odyssey infrared imaging system (LI-COR Biosciences, USA). β -actin was used as an internal control to assess equal loading. The relative expression level of each target protein was expressed as the ratio of target protein/ β -actin.^[12]

Statistical analysis

Continuous variables were presented as mean \pm standard deviation (SD) and analyzed using SPSS version 19.0 (IBM,

Armonk, NY, USA). The comparison among the data of multiple groups was performed by one-way analysis of variance and that of between the data of two groups was carried out by Student's *t*-test. Statistical significance was defined as $P < 0.05$.

RESULTS

Mouse model studies

Biological parameters

At the 12th week, body weight, Lee's index, abdominal fat index, perirenal fat index, periepididymal fat index, and kidney weight in the model group were all significantly higher than those in the control group [all $P < 0.05$; Table 1]. The mice used in our experiments were confirmed as C57BL/6J substrain mice by a genetic background identification of the samples [Supplementary Material 2]. Photographs of the mice in the model group and control group are shown in Supplementary Figure 1.

The mean serum cholesterol level in the model group significantly increased compared with that in the control group ($P < 0.01$). The mean serum triglyceride level in the model group also increased compared with that in the control group, but the difference had no statistical significance ($P = 0.12$). The mean blood glucose levels between these two groups had no statistically significant difference [$P = 0.28$; Table 2].

There was no difference in the mean nocturnal 12 h urinary protein excretion between the control and model groups at baseline ($678.2 \pm 219.8 \mu\text{g}$ vs. $638.4 \pm 137.0 \mu\text{g}$, $t = 0.407$,

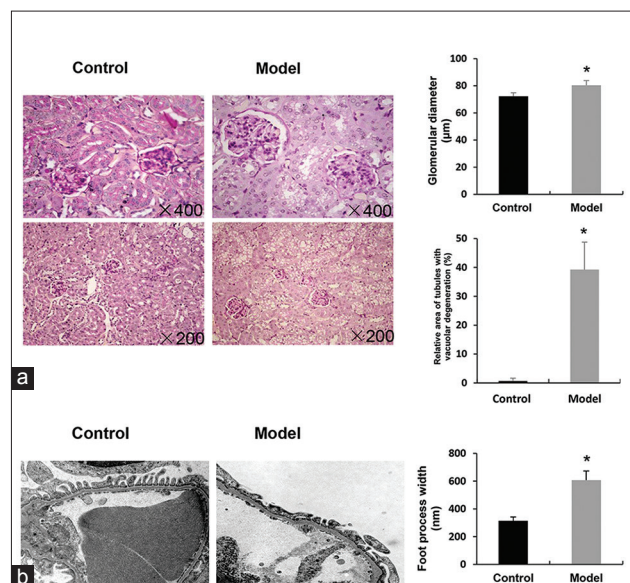


Figure 1: Renal histological changes. (a) Light microscopic images of renal cortex (PAS staining) and histograms showing average glomerular diameters and relative area of tubules with cytoplasmic vacuolar degeneration in the mice of ORG model group and control group. (b) Electron microscopic images of glomerulus (original magnification, $\times 20,000$) and histogram of average foot process width in the mice of the ORG model group and control group. Results are presented as mean \pm SD ($n = 7$ in each group). $*P < 0.01$ versus the control group. ORG: Obesity-related glomerulopathy; SD: Standard deviation.

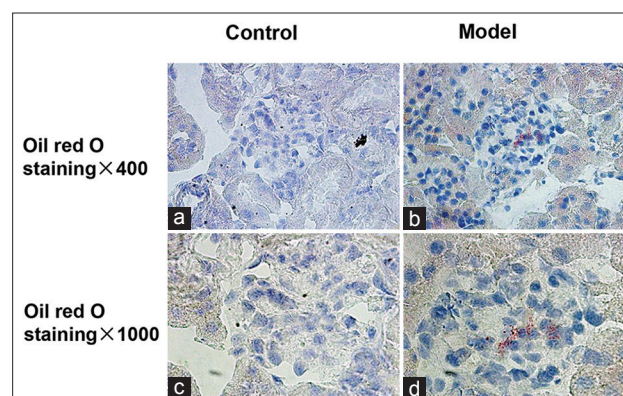


Figure 2: Glomerular lipid accumulation. Light microscopic images of oil red O staining on the renal cortex. Lipid accumulation in the glomerulus in the ORG model group (b and d) but not in the control group (a and c). ORG: Obesity-related glomerulopathy.

Table 1: Physical parameters measured at the end of the 12th week in this study

Parameters	Control group ($n = 7$)	Model group ($n = 7$)	<i>t</i>	<i>P</i>
Body weight (g)	26.7 \pm 1.0	34.7 \pm 2.0	-9.501	<0.01
Kidney weight (g)	0.33 \pm 0.03	0.39 \pm 0.02	-4.748	<0.01
Lee's index	2.99 \pm 0.07	3.18 \pm 0.10	-4.108	<0.01
Abdominal fat index (%)	0.92 \pm 0.19	1.55 \pm 0.15	-6.869	<0.01
Perirenal fat index (%)	0.50 \pm 0.22	1.06 \pm 0.48	-2.804	0.02
Periepididymal fat index (%)	1.71 \pm 0.60	3.09 \pm 1.32	-2.509	0.03

The data are shown as mean \pm SD. SD: Standard deviation.

$P = 0.69$), but at the 12th week, the mean nocturnal 12 h urinary protein excretion significantly increased in the model

group compared with that in the control group ($P < 0.01$). The mean CCr of the model group also significantly increased

Table 2: Biochemical parameters measured at the end of the 12th week in this study

Parameters	Control group (n = 7)	Model group (n = 7)	t	P
Serum cholesterol (mmol/L)	2.88 ± 0.30	4.05 ± 0.45	-5.682	<0.01
Serum triglyceride (mmol/L)	0.47 ± 0.15	0.68 ± 0.10	-2.958	0.12
Blood glucose (mmol/L)	9.14 ± 0.88	9.60 ± 0.61	-1.123	0.28
Urinary protein excretion (μg/nocturnal 12 h)	783.1 ± 187.7	1119.2 ± 182.9	-3.387	<0.01
Serum creatinine (μmol/L)	12.09 ± 1.74	12.20 ± 2.09	-1.111	0.91
Creatinine clearance rate (ml/min)	0.25 ± 0.09	0.44 ± 0.17	-2.644	0.02

The data are shown as mean ± SD. SD: Standard deviation.

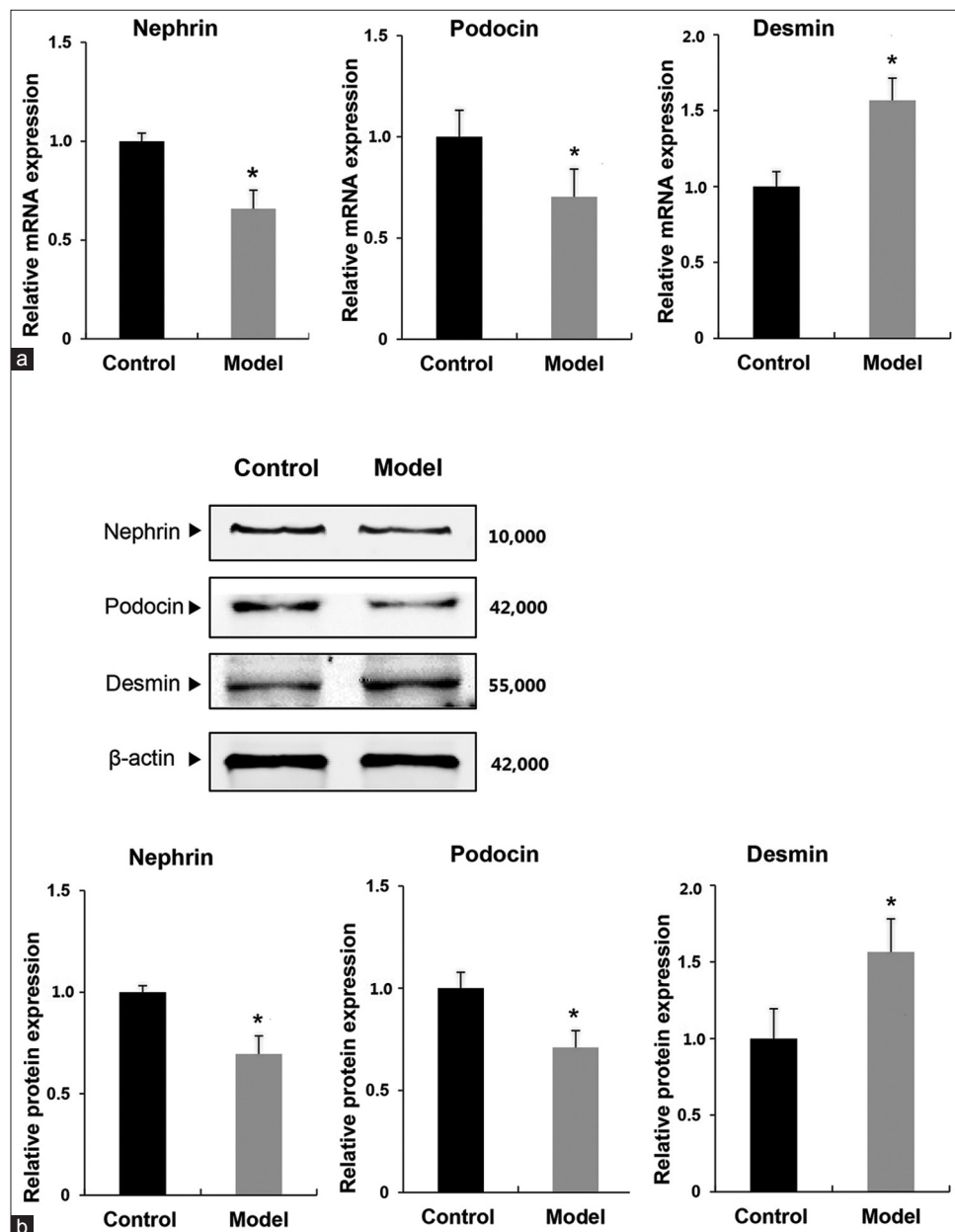


Figure 3: The mRNA and protein expression of podocyte-associated molecules in renal cortex tissue. (a) The relative mRNA expression of the podocyte-associated molecules including nephrin, podocin, and desmin measured by real-time quantitative PCR in ORG model group and control group. (b) The relative protein expression of the above podocyte-associated molecules detected by Western blot assay in ORG model group and control group. Results are presented as mean ± SD (n = 7 in each group). * $P < 0.01$ versus the control group. ORG: Obesity-related glomerulopathy; SD: Standard deviation.

compared with that in the control group ($P = 0.02$), but the mean serum creatinine levels between these two groups had no statistically significant difference ($P = 0.91$; Table 2).

Glomerular diameter

The mean glomerular diameter in the model group was significantly longer than that in the control group at the end of the 12th week ($80.36 \pm 3.42 \mu\text{m}$ vs. $72.26 \pm 2.61 \mu\text{m}$, $t = -5.798$, $P < 0.01$; Figure 1a).

Relative area of tubules with cytoplasmic vacuolar degeneration

The relative area of tubules with cytoplasmic vacuolar degeneration in the model group was significantly larger than that

in the control group at the end of the 12th week ($39.0\% \pm 9.5\%$ vs. $0.65\% \pm 0.98\%$, $t = -10.655$, $P < 0.01$; Figure 1a).

Foot process width

Under transmission electron microscope, there was mild and segmental foot process effacement in the model group and the mean foot process width in the model group was significantly wider than that in the control group at the end of the 12th week ($607.80 \pm 67.23 \text{ nm}$ vs. $313.80 \pm 27.81 \text{ nm}$, $t = -10.815$, $P < 0.01$; Figure 1b).

Lipid accumulation in glomerulus

The results of oil red O staining revealed that there were some lipid droplets in the glomeruli of

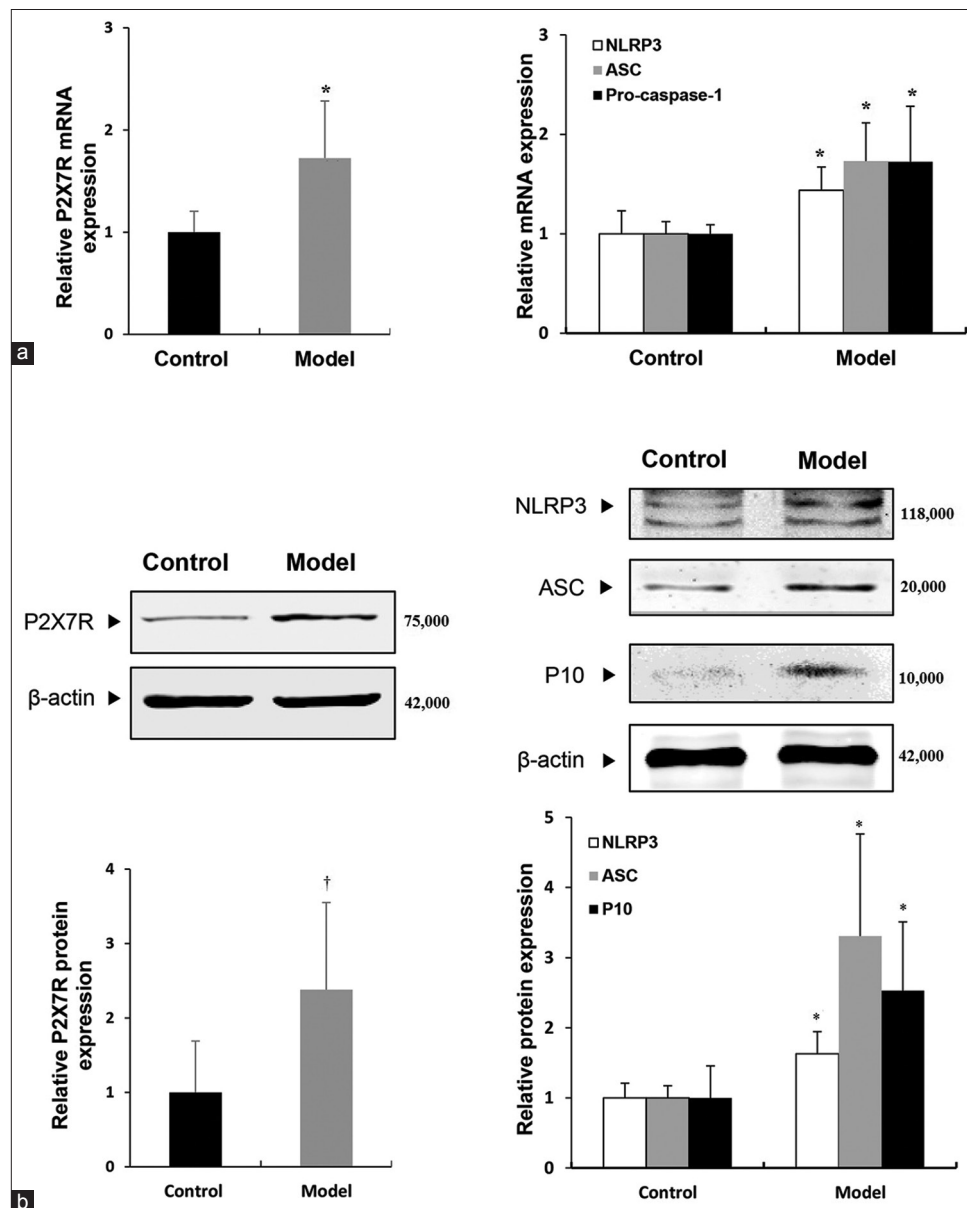


Figure 4: The mRNA and protein expression of P2X7R and NLRP3 inflammasome components in the renal cortex tissue. (a) The relative mRNA expression of P2X7R and the NLRP3 inflammasome components including NLRP3, ASC, and pro-caspase-1 tested by real-time quantitative PCR in ORG model group and control group. (b) The relative protein expression of P2X7R and the NLRP3 inflammasome components including NLRP3, ASC, and active caspase-1 subunit p10 detected by Western blot assay in ORG model group and control group. Results are presented as mean \pm SD ($n = 7$ in each group). * $P < 0.01$ or † $P < 0.05$ versus the control group. NLRP3: Nucleotide-binding and oligomerization domain-like receptor protein 3; ASC: Apoptosis-associated speck-like protein containing CARD; ORG: Obesity-related glomerulopathy; P2X7R: Purinergic 2X7 receptor; SD: Standard deviation.

mice in the ORG group, but not in the control group [Figure 2].

Expression of podocyte-associated molecules

The podocyte-associated molecules detected in this study included nephrin, podocin, and desmin (a sensitive marker of podocyte damage^[13]). Real time-PCR and Western blot assay, which were conducted using the RNA and protein extracted from renal cortex tissue, showed that the mRNA and protein expression of nephrin (mRNA: $t = 8.711$, $P < 0.01$; protein: $t = 8.501$, $P < 0.01$) and podocin (mRNA: $t = 4.143$, $P < 0.01$; protein: $t = 6.678$, $P < 0.01$) were significantly downregulated, and the mRNA ($t = -8.574$, $P < 0.01$) and protein ($t = -5.161$, $P < 0.01$) expression of desmin were significantly upregulated in the model group, compared with that of the control group [Figure 3]. These results suggested that podocytes were damaged in the mouse model.

Expression of purinergic 2X7 receptor/nucleotide-binding and oligomerization domain-like receptor protein 3 inflammasome components

Real time-PCR and Western blot assay, which were conducted using the same extracts mentioned above, showed that the mRNA and protein expression of P2X7R (mRNA: $t = -3.200$, $P < 0.01$; protein: $t = -2.678$, $P = 0.02$) and NLRP3 inflammasome components including NLRP3 (mRNA: $t = -3.503$, $P < 0.01$; protein: $t = -4.407$, $P < 0.01$), ASC (mRNA: $t = -4.798$, $P < 0.01$; protein: $t = -4.166$, $P < 0.01$), and caspase-1 (pro-caspase-1 mRNA in gene level: $t = -3.395$, $P < 0.01$; active caspase-1 subunit p10 in protein level: $t = -3.697$, $P < 0.01$) were significantly upregulated in the model group, compared with that of the control group [Figure 4]. These results suggested that the expression of P2X7R/NLRP3 inflammasome was enhanced and the NLRP3 inflammasome was activated in the renal cortex tissue of the mouse model.

Location of purinergic 2X7 receptor and nucleotide-binding and oligomerization domain-like receptor protein 3 in podocytes of obesity-related glomerulopathy mouse model

Confocal microscopy can show whether P2X7R or NLRP3 is co-localized with nephrin so as to determine whether P2X7R or NLRP3 locates on podocytes. The results revealed that P2X7R and NLRP3 were expressed within glomeruli at a low level and very little co-localization with nephrin could be observed in the mice of control group, but the region of their expression within glomeruli, especially on podocytes, was obviously expanded in the mice of model group [Figure 5]. However, outside of glomeruli, there was hardly any expression of P2X7R and NLRP3. These results suggested that the higher expression of P2X7R and NLRP3 detected by real-time PCR and Western blot assay in the extracts of renal cortex in ORG mice reflected, to a large extent, their higher expression in podocytes.

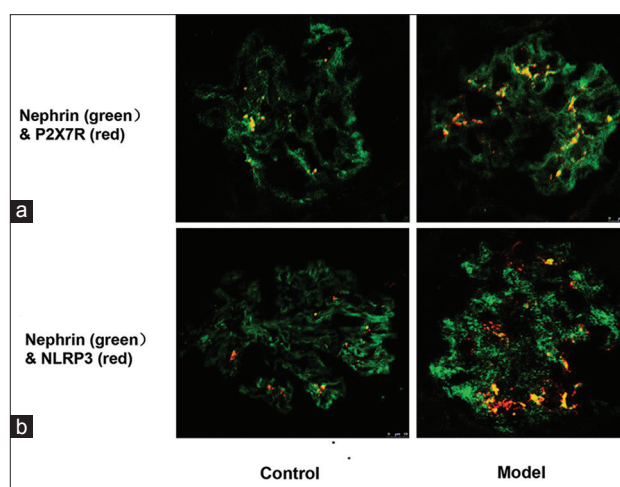


Figure 5: Confocal microscopy of P2X7R and nephrin or NLRP3 and nephrin in the renal cortex. (a) Confocal microscopic images of P2X7R (red) with nephrin (green) in the renal cortex (original magnification, $\times 1000$). (b) Confocal microscopic image of NLRP3 (red) with nephrin (green) in the renal cortex section (original magnification, $\times 1000$). Yellow color indicates co-localization.

Cellular experiments

Effects of KN-62 on the expression of purinergic 2X7 receptor/nucleotide-binding and oligomerization domain-like receptor protein 3 inflammasome components as well as podocyte-associated molecules

To verify the possible pathogenic role of P2X7R in podocyte damage of ORG, cellular experiments *in vitro* were performed in which podocytes were incubated with leptin alone or leptin plus KN-62, a P2X7R antagonist. The concentrations of leptin and KN-62 used in the experiments were defined by LDH release assays [Supplementary Material 2 and Supplementary Figure 2].

The results showed that the mRNA and protein expression of P2X7R (mRNA: $t = -5.514$, $P < 0.01$; protein: $t = -4.436$, $P < 0.01$) and NLRP3 inflammasome components including NLRP3 (mRNA: $t = -3.582$, $P < 0.01$; protein: $t = -7.948$, $P < 0.01$), ASC (mRNA: $t = -5.128$, $P < 0.01$; protein: $t = -8.950$, $P < 0.01$), and caspase-1 (mRNA: $t = -3.634$, $P = 0.02$; protein: $t = -2.722$, $P < 0.01$) were significantly upregulated in the leptin group, compared with the control group [Figure 6]. These results suggested that the expression of P2X7R/NLRP3 inflammasome was enhanced and the NLRP3 inflammasome was activated in the cultured podocytes treated by leptin.

However, the mRNA and protein expression of P2X7R (mRNA: 1.194 ± 0.289 vs. 2.098 ± 0.274 , $t = 4.454$, $P < 0.01$; protein: P2X7R 1.126 ± 0.275 vs. 1.976 ± 0.518 , $t = 3.856$, $P = 0.01$) and NLRP3 inflammasome components (NLRP3: mRNA: 0.841 ± 0.254 vs. 1.618 ± 0.287 , $t = 4.504$, $P < 0.01$; protein: 1.197 ± 0.132 vs. 1.684 ± 0.201 , $t = 5.665$, $P < 0.01$; ASC: mRNA: 0.893 ± 0.177 vs. 1.702 ± 0.231 , $t = 6.526$, $P < 0.01$; protein: 1.272 ± 0.173 vs. 2.016 ± 0.242 , $t = -6.553$, $P < 0.01$; caspase-1: 0.825 ± 0.129 vs. 1.463 ± 0.351 , $t = 5.012$, $P < 0.01$; protein: 1.425 ± 0.121 vs. 2.433 ± 0.311 ,

$t = -1.908, P < 0.01$) were significantly downregulated in the leptin plus KN-62 group, compared with that of the leptin group [Figure 6].

In addition, the expression of podocyte-associated molecules also simultaneously changed. Leptin significantly downregulated the mRNA and protein expression of nephrin (mRNA: $t = 5.686, P < 0.01$; protein: $t = 3.379, P < 0.01$) and podocin (mRNA: $t = 4.128, P < 0.01$; protein: $t = 7.483, P < 0.01$) and upregulated the mRNA and protein expression of desmin (mRNA: $t = -4.896, P < 0.01$; protein: $t = -4.696, P < 0.01$), compared with that of the control group [Figure 7].

However, KN-62 significantly reversed the above changes resulted from leptin in the podocyte-associated molecular expression at both mRNA and protein levels (mRNA: nephrin, 0.708 ± 0.167 vs. $0.456 \pm 0.117, t = -2.636, P = 0.01$; podocin,

0.877 ± 0.074 vs. $0.645 \pm 0.095, t = -2.703, P = 0.02$; and desmin, 1.195 ± 0.168 vs. $1.532 \pm 0.168, t = 3.100, P = 0.05$; protein: nephrin, 0.973 ± 0.203 vs. $0.508 \pm 0.107, t = -3.193, P < 0.01$; podocin, 0.811 ± 0.095 vs. $0.499 \pm 0.035, t = -4.655, P < 0.01$; and desmin, 1.222 ± 0.455 vs. $2.142 \pm 0.498, t = 3.779, P = 0.02$) [Figure 7].

Effects of A438079 on the expression of purinergic 2X7 receptor/nucleotide-binding and oligomerization domain-like receptor protein 3 inflammasome components as well as podocyte-associated molecules

To further confirm the possible pathogenic role of P2X7R in podocyte damage of ORG, A438079, a highly selective P2X7R antagonist, was also used for the cell experiments of podocytes *in vitro*. The experimental concentration of A438079 was also defined by LDH release assays [Supplementary Material 2]. All the experimental

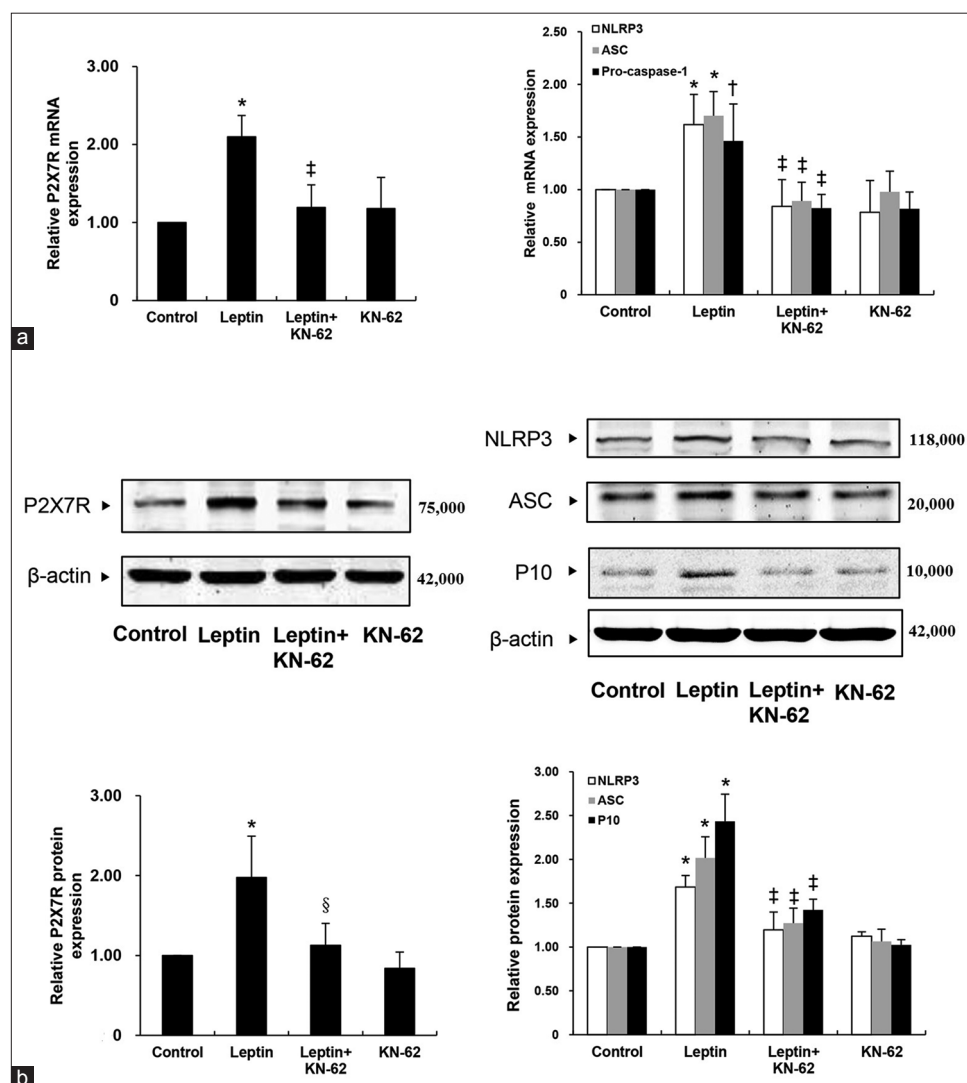


Figure 6: Effects of KN-62 on the expression of P2X7R and NLRP3 inflammasome components in the cultured podocytes. (a) After 4 h and 12 h of incubation, the mRNA expression of P2X7R and NLRP3 inflammasome components (NLRP3, ASC, and pro-caspase-1) was detected by real-time quantitative PCR. (b) After 6 h and 24 h of incubation, the protein expression of P2X7R and NLRP3 inflammasome components (NLRP3, ASC, and active caspase-1 subunit p10) was detected by Western blot analysis. Results are presented as mean \pm SD ($n = 4$). * $P < 0.01$ or † $P < 0.05$ versus the control group. ‡ $P < 0.01$ or § $P < 0.05$ versus the leptin group. NLRP3: Nucleotide-binding and oligomerization domain-like receptor protein 3; ASC: Apoptosis-associated speck-like protein containing CARD; P2X7R: Purinergic 2X7 receptor; SD: Standard deviation.

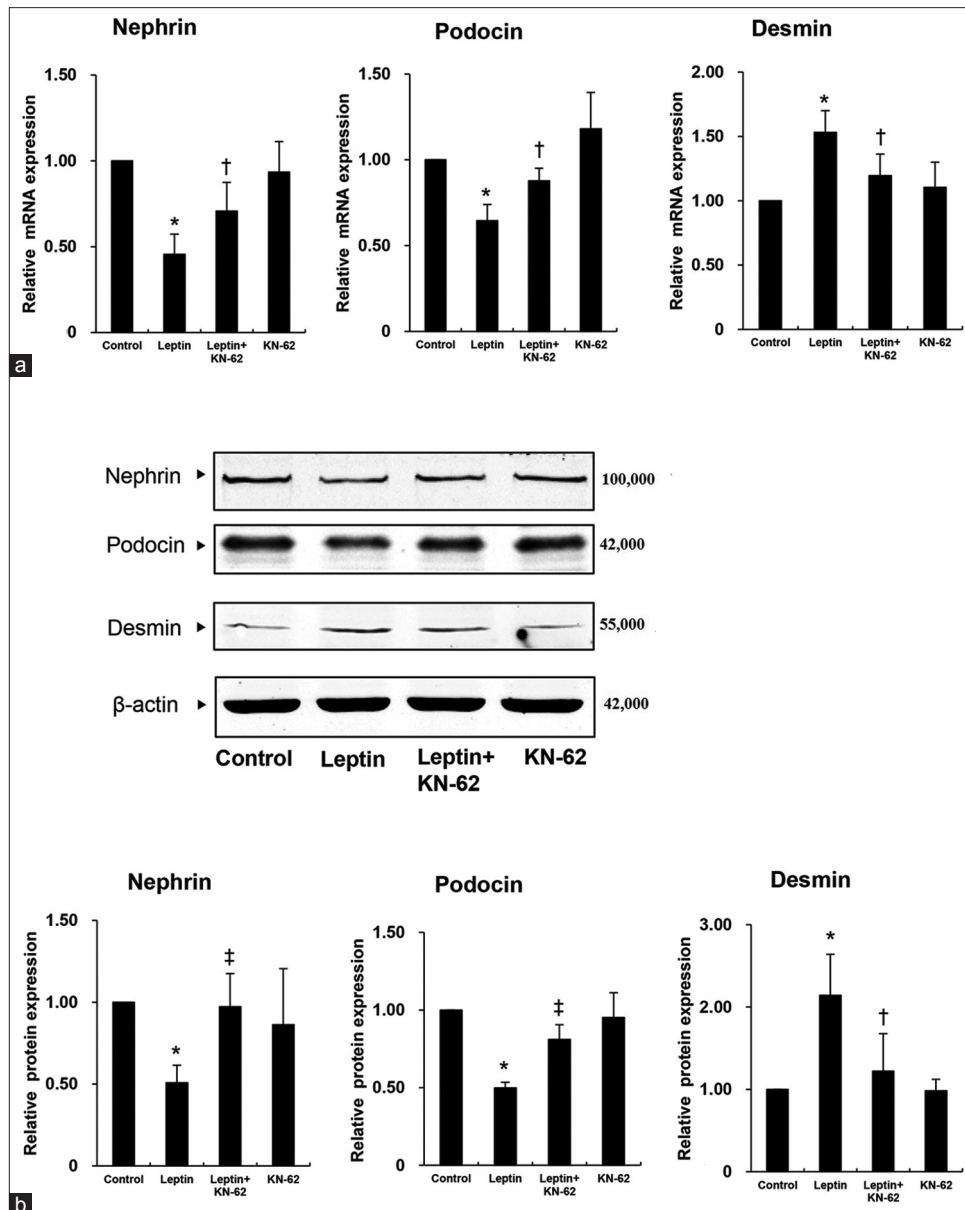


Figure 7: Effects of KN-62 on the expression of podocyte-associated molecules in the cultured podocytes. (a) After 12 h of incubation, the mRNA expression of podocyte-associated molecules including nephrin, podocin, and desmin was detected by real-time quantitative PCR. (b) After 24 h of incubation, the protein expression of nephrin, podocin, and desmin was detected by Western blot assay. Results are presented as mean \pm SD ($n = 4$). * $P < 0.01$ versus the control group. † $P < 0.05$ or ‡ $P < 0.01$ versus the leptin group.

results, i.e., the effects of A438079 on the expression of P2X7R/NLRP3 inflammasome components as well as podocyte-associated molecules, were very similar to those in the experiments carried out with KN-62 [Figures 8 and 9].

DISCUSSION

Podocyte damage and dysfunction are the hallmarks of ORG. The following renal pathological changes are often observed: increased foot process width, mild and segmental foot process effacement, decreased podocyte density and number, even podocyte detachment from basement membrane, etc., Furthermore, the severity of podocyte damage is closely correlated with the degree of proteinuria and renal dysfunction. It has been generally recognized that

podocyte damage and dysfunction play a pivotal role in the occurrence and progression of ORG.^[11-13,22]

Animal model and cell model are important tools for studying the pathogenesis of disease. This study successfully established a mouse model of ORG by HFD feeding. The mice in the model group presented the following characteristics: (1) obesity with significantly increased body weight, Lee's index, abdominal fat index, perirenal fat index, and periepididymal fat index; (2) significantly increased urine protein excretion and CCR; (3) glomerulomegaly with lipid accumulation in glomeruli; and (4) podocyte damage showing significantly increased foot process width, mild segmental foot process effacement, and altered expression of podocyte-associated molecules. In addition, this study also

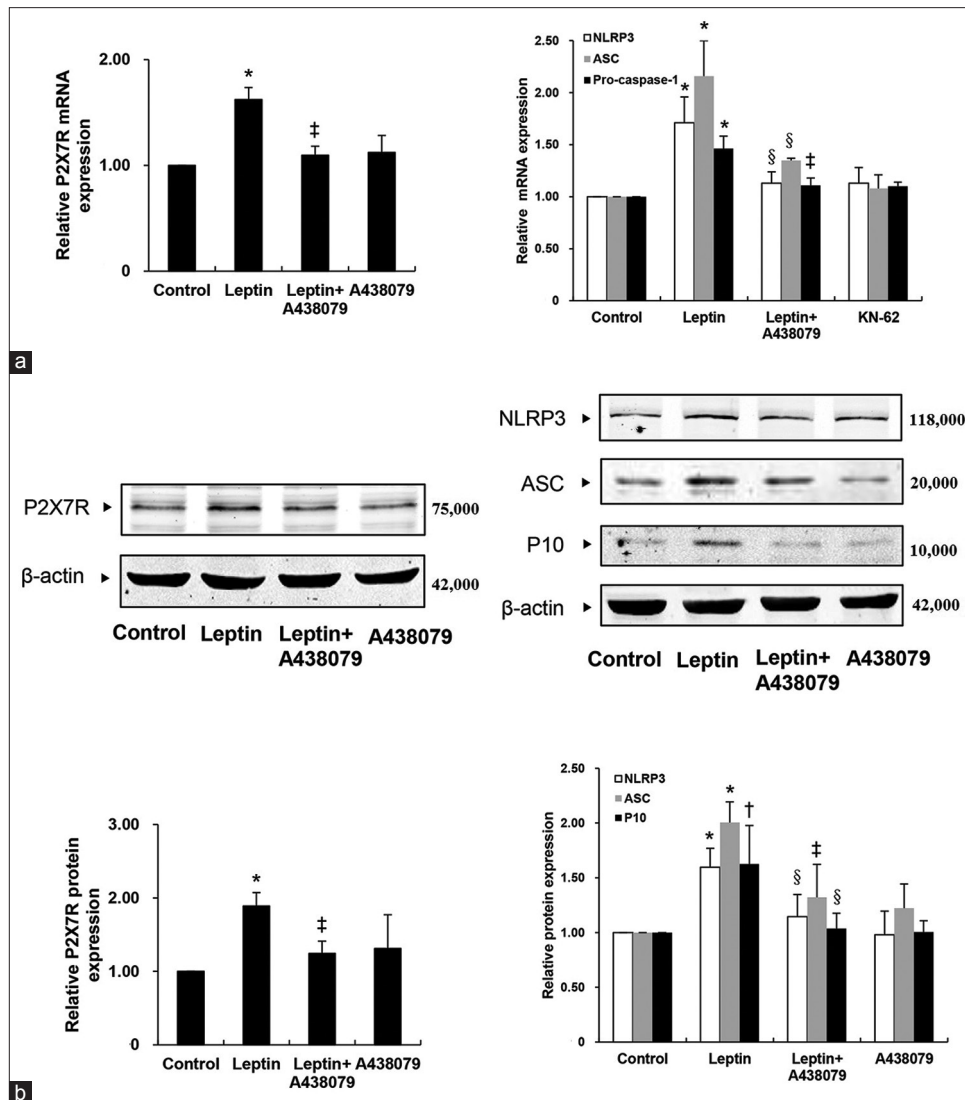


Figure 8: Effects of A438079 on the expression of P2X7R and NLRP3 inflammasome components in the cultured podocytes. (a) After 4 h and 12 h of incubation, the mRNA expression of P2X7R and NLRP3 inflammasome components (NLRP3, ASC, and pro-caspase-1) was detected by real-time quantitative PCR. (b) After 6 h and 24 h of incubation, the protein expression of P2X7R and NLRP3 inflammasome components (NLRP3, ASC, and active caspase-1 subunit p10) was detected by Western blot assay. Results are presented as mean \pm SD ($n = 4$). * $P < 0.01$ or $^{\dagger}P < 0.05$ versus the control group; $^{\ddagger}P < 0.01$ or $^{\S}P < 0.05$ versus the leptin group. NLRP3: Nucleotide-binding and oligomerization domain-like receptor protein 3; ASC: Apoptosis-associated speck-like protein containing CARD; P2X7R: Purinergic 2X7 receptor; SD: Standard deviation.

successfully established a cell model of podocyte damage caused by leptin. Leptin is one of the important adipokines predominantly secreted by adipocytes. Accumulating data have shown that hyperleptinemia often occurred in obese individuals and could induce a lot of pathophysiologic responses which were involved in the inflammatory effect and kidney damage, including podocyte damage, of ORG.^[12,13,23-26] Therefore, leptin was selected as the inducer to the established cell model in this study. Both animal and cell models provided this study with good platforms for research of pathogenic mechanism of ORG *in vivo* and *in vitro*.

The pathogenic mechanism of ORG has not yet been fully elucidated, and it is possible that many factors are involved in ORG pathogenesis.^[22,25] Obesity often creates a low-level chronic inflammatory state called as metaflammation,

which can facilitate the occurrence and progression of obesity-related diseases, including ORG.^[25,27-29] Moreover, it was also reported that NLRP3 inflammasome participated in the obesity-induced metaflammation.^[29-31] Hence, this study chose the pathogenic role of inflammation in ORG as the research subject, especially focusing on the pathogenic role of activated NLRP3 inflammasome in podocyte damage.

In 2012, Zhang *et al.*^[32] first demonstrated that podocytes could express all the key components of NLRP3 inflammasome (NLRP3, ASC, and caspase 1), and the formation and activation of NLRP3 inflammasome in podocytes could in turn contribute to podocyte damage in a mouse model of hyperhomocysteinemia. Afterward, in 2014, Boini *et al.*^[33] successfully made a mouse model of obesity-associated glomerular injury by feeding HFD and

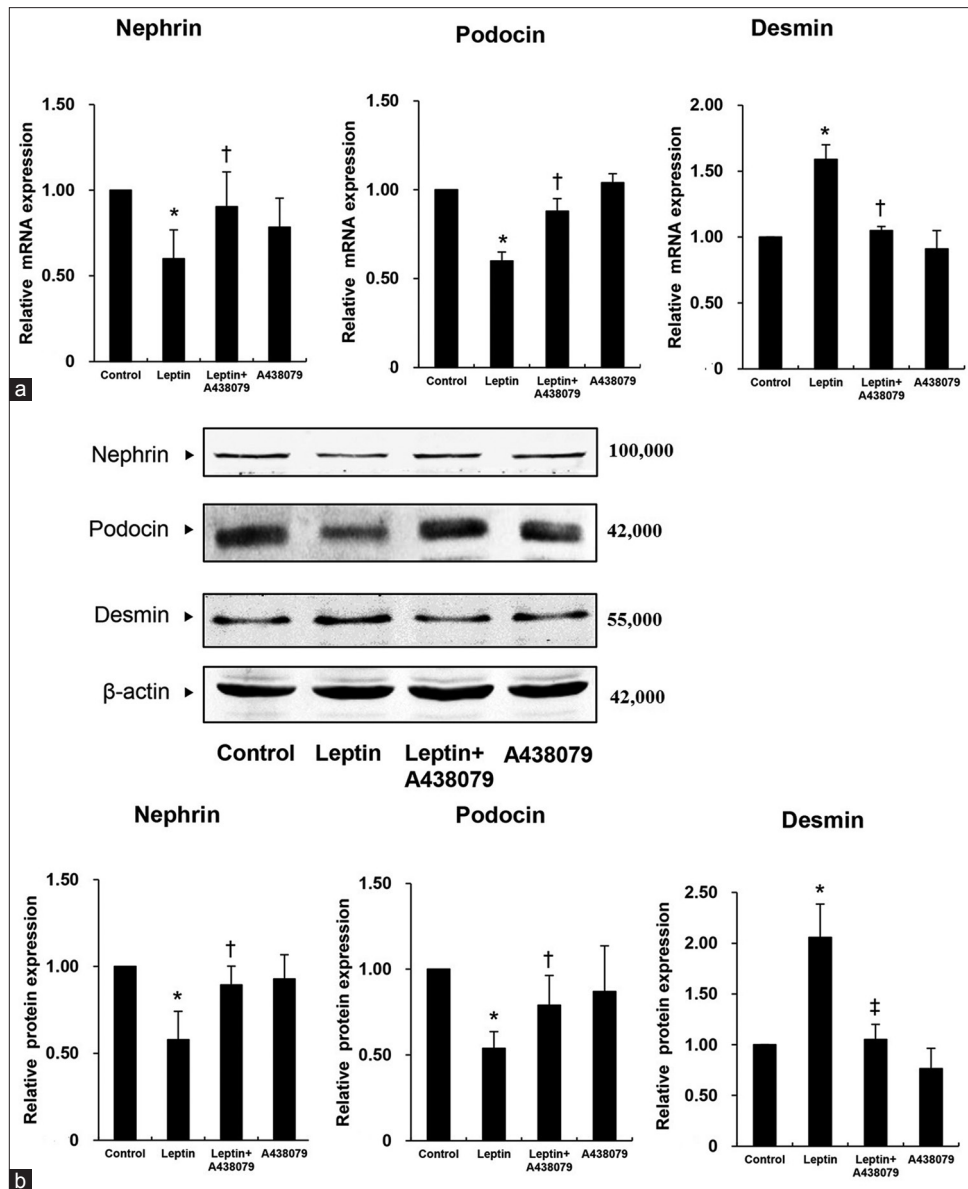


Figure 9: Effects of A438079 on the expression of podocyte-associated molecules in the cultured podocytes. (a) After 12 h of incubation, the mRNA expression of podocyte-associated molecules including nephrin, podocin, and desmin was detected by real-time quantitative PCR. (b) After 24 h of incubation, the protein expression of nephrin, podocin, and desmin was detected by Western blot assay. Results are presented as mean \pm SD ($n = 4$). * $P < 0.01$ versus the control group; † $P < 0.05$ or ‡ $P < 0.01$ versus the leptin group.

found the formation and activation of NLRP3 inflammasome in the podocytes of these mice. More importantly, *ASC* gene deletion or intrarenal *ASC* gene silencing could significantly block the above changes of NLRP3 inflammasome in podocytes and consequently attenuate the podocyte damage and proteinuria. These results suggested that the formation and activation of NLRP3 inflammasome in podocytes might play an important role in the development of obesity-associated glomerular injury.^[33] The *in vivo* and *in vitro* results of this study both supported the above findings and further confirmed the pathogenic role of activated NLRP3 inflammasome in ORG. However, Boini *et al.*^[33] did not explore whether the upstream molecule of NLRP3 inflammasome, P2X7R, was also involved in the podocyte damage of ORG.

P2X7R is an extracellular, ATP-gated, nonselective cation channel with multiple functions.^[17,34,35] One of its most important functions is to activate NLRP3 inflammasome, and it has been even considered to be central in the activation of NLRP3 inflammasome.^[35,36] P2X7R is widely distributed in a variety of cells, including podocytes.^[34,35,37] We speculated that P2X7R in podocytes might play a critical role in the pathogenesis of ORG by activating NLRP3 inflammasome in podocyte, so the present study was carried out to verify this hypothesis. This research on cultured podocytes showed that the upregulated P2X7R expression induced by leptin was accompanied with NLRP3 inflammasome activation and podocyte damage (presented as expression changes of podocyte-associated molecules). Furthermore, both P2X7R antagonists, KN-62 (a noncompetitive antagonist of P2X7R

and antagonist of Ca²⁺/calmodulin-dependent protein kinase II^[38]) and A438079 (a potent and highly selective antagonist of P2X7R^[38]), could significantly attenuate all the above changes. The results of cell experiments *in vitro*, combined with the results of mouse model *in vivo*, suggested that P2X7R was involved in the podocyte damage of ORG via activation of NLRP3 inflammasome.

The exact mechanism by which activated NLRP3 inflammasome results in podocyte damage is still unclear. It might be related to the production of inflammatory cytokines such as IL-1 β and IL-18 after NLRP3 inflammasome activation, which might act in an autocrine or paracrine fashion to induce podocyte damage and/or dysfunction; for example, reduction of nephrin production.^[33,39] It was also probably related to the noninflammatory effects of NLRP3 inflammasome, such as pyroptotic cell death, cytoskeleton changes, and alterations of cell metabolism.^[33,40] However, accurate pathogenic mechanism still needs to be explored in the future.

In this study, we did not carry out an experiment *in vivo* on the mice with P2X7R gene deletion or gene silence and did not observe the effects of such intervention on preventing ORG, including blocking NLRP3 inflammasome activation and attenuating podocyte damage. This was a deficiency of our study. We will perform a further study in the future.

In conclusion, the present study suggested that P2X7R can trigger NLRP3 inflammasome activation, and P2X7R/NLRP3 inflammasome activation might be involved in the pathogenesis of ORG. Hence, targeting the P2X7R/NLRP3 inflammasome pathway might be useful for the prevention and treatment of ORG.

Supplementary information is linked to the online version of the paper on the Chinese Medical Journal website.

Financial support and sponsorship

This research work was supported by grants from the National Natural Science Foundation of China (No. 81573745 and No. 8160140274), Beijing Municipal Natural Science Foundation (No. 7172066), and Beijing Development Foundation of Traditional Chinese Medicine (QN2016-23).

Conflicts of interest

There are no conflicts of interest.

REFERENCES

1. Arroyo-Johnson C, Mincey KD. Obesity epidemiology worldwide. *Gastroenterol Clin North Am* 2016;45:571-9. doi: 10.1016/j.gtc.2016.07.012.
2. Chertow GM, Hsu CY, Johansen KL. The enlarging body of evidence: Obesity and chronic kidney disease. *J Am Soc Nephrol* 2006;17:1501-2. doi: 10.1681/ASN.2006040327.
3. de Vries AP, Ruggenenti P, Ruan XZ, Praga M, Cruzado JM, Bajema IM, *et al*. Fatty kidney: Emerging role of ectopic lipid in obesity-related renal disease. *Lancet Diabetes Endocrinol* 2014;2:417-26. doi: 10.1016/S2213-8587(14)70065-8.
4. Weisinger JR, Kempson RL, Eldridge FL, Swenson RS. The nephrotic syndrome: A complication of massive obesity. *Ann Intern Med* 1974;81:440-7. doi: 10.7326/0003-4189-81-4-440.
5. Kambham N, Markowitz GS, Valeri AM, Lin J, D'Agati VD. Obesity-related glomerulopathy: An emerging epidemic. *Kidney Int* 2001;59:1498-509. doi: 10.1046/j.15231755.2001.0590041498.x.
6. Cheng H, Dong HR, Lin RQ, Sun LJ, Chen YP. Determination of normal value of glomerular size in Chinese adults by different measurement methods. *Nephrology (Carlton)* 2012;17:488-92. doi: 10.1111/j.1440-1797.2012.01606.x.
7. Zhang HJ, Cheng H, Yang M, Liu ZS, Chen YP. Correlation analysis between serum α -klotho level and the development of obesity-related glomerulopathy. *Chin J Nephrol* 2017;33:410-5. doi: 10.3760/cma.j.issn.1001-7097.2017.06.002.
8. Jarad G, Miner JH. Update on the glomerular filtration barrier. *Curr Opin Nephrol Hypertens* 2009;18:226-32. doi: 10.1097/MNH.0b013e3283296044.
9. Grahammer F. New structural insights into podocyte biology. *Cell Tissue Res* 2017;369:5-10. doi: 10.1007/s00441-017-2590-3.
10. Camici M, Galetta F, Abraham N, Carpi A. Obesity-related glomerulopathy and podocyte injury: A mini review. *Front Biosci (Elite Ed)* 2012;4:1058-70.
11. Chen HM, Liu ZH, Zeng CH, Li SJ, Wang QW, Li LS, *et al*. Podocyte lesions in patients with obesity-related glomerulopathy. *Am J Kidney Dis* 2006;48:772-9. doi: 10.1053/j.ajkd.2006.07.025.
12. Liu BL, Chen YP, Cheng H, Wang YY, Rui HL, Yang M, *et al*. The protective effects of curcumin on obesity-related glomerulopathy are associated with inhibition of Wnt/ β -catenin signaling activation in podocytes. *Evid Based Complement Alternat Med* 2015;2015:827472. doi: 10.1155/2015/827472.
13. Chen JY, Jian DY, Lien CC, Lin YT, Ting CH, Chen LK, *et al*. Adipocytes play an etiological role in the podocytopathy of high-fat diet-fed rats. *J Endocrinol* 2016;231:109-20. doi: 10.1530/JOE-16-0064.
14. Schroder K, Tschopp J. The inflammasomes. *Cell* 2010;140:821-32. doi: 10.1016/j.cell.2010.01.040.
15. Sutterwala FS, Ogura Y, Zamboni DS, Roy CR, Flavell RA. NALP3: A key player in caspase-1 activation. *J Endotoxin Res* 2006;12:251-6. doi: 1177/09680519060120040701.
16. Cassel SL, Joly S, Sutterwala FS. The NLRP3 inflammasome: A sensor of immune danger signals. *Semin Immunol* 2009;21:194-8. doi: 10.1016/j.smim.2009.05.002.
17. Solini A, Menini S, Rossi C, Ricci C, Santini E, Blasetti Fantauzzi C, *et al*. The purinergic 2X7 receptor participates in renal inflammation and injury induced by high-fat diet: Possible role of NLRP3 inflammasome activation. *J Pathol* 2013;231:342-53. doi: 10.1002/path.4237.
18. Riteau N, Gasse P, Fauconnier L, Gombault A, Couegnat M, Fick L, *et al*. Extracellular ATP is a danger signal activating P2X7 receptor in lung inflammation and fibrosis. *Am J Respir Crit Care Med* 2010;182:774-83. doi: 10.1164/rccm.201003-0359OC.
19. Schorn C, Frey B, Lauber K, Janko C, Strysió M, Keppeler H, *et al*. Sodium overload and water influx activate the NALP3 inflammasome. *J Biol Chem* 2011;286:35-41. doi: 10.1074/jbc.M110.139048.
20. Koop K, Eikmans M, Baelde HJ, Kawachi H, De Heer E, Paul LC, *et al*. Expression of podocyte-associated molecules in acquired human kidney diseases. *J Am Soc Nephrol* 2003;14:2063-71. doi: 10.1097/01.ASN.0000078803.53165.C9.
21. Boini KM, Xia M, Xiong J, Li C, Payne LP, Li PL. Implication of CD38 gene in podocyte epithelial-to-mesenchymal transition and glomerular sclerosis. *J Cell Mol Med* 2012;16:1674-85. doi: 10.1111/j.1582-4934.2011.01462.x.
22. D'Agati VD, Chagnac A, de Vries AP, Levi M, Porrini E, Herman-Edelstein M, *et al*. Obesity-related glomerulopathy: Clinical and pathologic characteristics and pathogenesis. *Nat Rev Nephrol* 2016;12:453-71. doi: 10.1038/nrneph.2016.75.
23. Hoffer U, Hobbie K, Wilson R, Bai R, Rahman A, Malarkey D, *et al*. Diet-induced obesity is associated with hyperleptinemia, hyperinsulinemia, hepatic steatosis, and glomerulopathy in C57Bl/6J mice. *Endocrine* 2009;36:311-25. doi: 10.1007/s12020-009-9224-9.
24. Briffa JF, McAinch AJ, Poronnik P, Hryciw DH. Adipokines as a link between obesity and chronic kidney disease. *Am J Physiol Renal Physiol* 2013;305:F1629-36. doi: 10.1152/ajprenal.00263.2013.
25. Tang J, Yan H, Zhuang S. Inflammation and oxidative stress in obesity-related glomerulopathy. *Int J Nephrol* 2012;2012:608397. doi: 10.1155/2012/608397.

26. Papafragkaki DK, Tolis G. Obesity and renal disease: A possible role of leptin. *Hormones (Athens)* 2005;4:90-5.
27. Snyder S, Turner GA, Turner A. Obesity-related kidney disease. *Prim Care* 2014;41:875-93. doi: 10.1016/j.pop.2014.08.008.
28. Imig JD, Ryan MJ. Immune and inflammatory role in renal disease. *Compr Physiol* 2013;3:957-76. doi: 10.1002/cphy.c120028.
29. Mastrocola R, Aragno M, Alloatti G, Collino M, Penna C, Pagliaro P. Metaflammation: Tissue-specific alterations of the NLRP3 inflammasome platform in metabolic syndrome. *Curr Med Chem* 2018;25:1294-310. doi: 10.2174/0929867324666170407123522.
30. Vandanmagsar B, Youm YH, Ravussin A, Galgani JE, Stadler K, Mynatt RL, *et al.* The NLRP3 inflammasome instigates obesity-induced inflammation and insulin resistance. *Nat Med* 2011;17:179-88. doi: 10.1038/nm.2279.
31. Chang A, Ko K, Clark MR. The emerging role of the inflammasome in kidney diseases. *Curr Opin Nephrol Hypertens* 2014;23:204-10. doi: 10.1097/01.mnh.0000444814.49755.90.
32. Zhang C, Boini KM, Xia M, Abais JM, Li X, Liu Q, *et al.* Activation of nod-like receptor protein 3 inflammasomes turns on podocyte injury and glomerular sclerosis in hyperhomocysteinemia. *Hypertension* 2012;60:154-62. doi: 10.1161/HYPERTENSIONAHA.111.189688.
33. Boini KM, Xia M, Abais JM, Li G, Pitzer AL, Gehr TW, *et al.* Activation of inflammasomes in podocyte injury of mice on the high fat diet: Effects of ASC gene deletion and silencing. *Biochim Biophys Acta* 2014;1843:836-45. doi: 10.1016/j.bbamcr.2014.01.033.
34. Vonend O, Turner CM, Chan CM, Loesch A, Dell'Anna GC, Srai KS, *et al.* Glomerular expression of the ATP-sensitive P2X receptor in diabetic and hypertensive rat models. *Kidney Int* 2004;66:157-66. doi: 10.1111/j.1523-1755.2004.00717.x.
35. Zhao J, Wang H, Dai C, Wang H, Zhang H, Huang Y, *et al.* P2X7 blockade attenuates murine lupus nephritis by inhibiting activation of the NLRP3/ASC/caspase 1 pathway. *Arthritis Rheum* 2013;65:3176-85. doi: 10.1002/art.38174.
36. Bours MJ, Dagnelie PC, Giuliani AL, Wesselius A, Di Virgilio F. P2 receptors and extracellular ATP: A novel homeostatic pathway in inflammation. *Front Biosci (Schol Ed)* 2011;3:1443-56.
37. Fischer KG, Saueressig U, Jacobshagen C, Wichelmann A, Pavenstädt H. Extracellular nucleotides regulate cellular functions of podocytes in culture. *Am J Physiol Renal Physiol* 2001;281:F1075-81. doi: 10.1152/ajprenal.2001.281.6.F1075.
38. North RA, Jarvis MF. P2X receptors as drug targets. *Mol Pharmacol* 2013;83:759-69. doi: 10.1124/mol.112.083758.
39. Takano Y, Yamauchi K, Hayakawa K, Hiramatsu N, Kasai A, Okamura M, *et al.* Transcriptional suppression of nephrin in podocytes by macrophages: Roles of inflammatory cytokines and involvement of the PI3K/Akt pathway. *FEBS Lett* 2007;581:421-6. doi: 10.1016/j.febslet.2006.12.051.
40. Lamkanfi M. Emerging inflammasome effector mechanisms. *Nat Rev Immunol* 2011;11:213-20. doi: 10.1038/nri2936.

P2X7R通过活化NLRP3炎症体参与肥胖相关性肾小球病的足细胞损伤

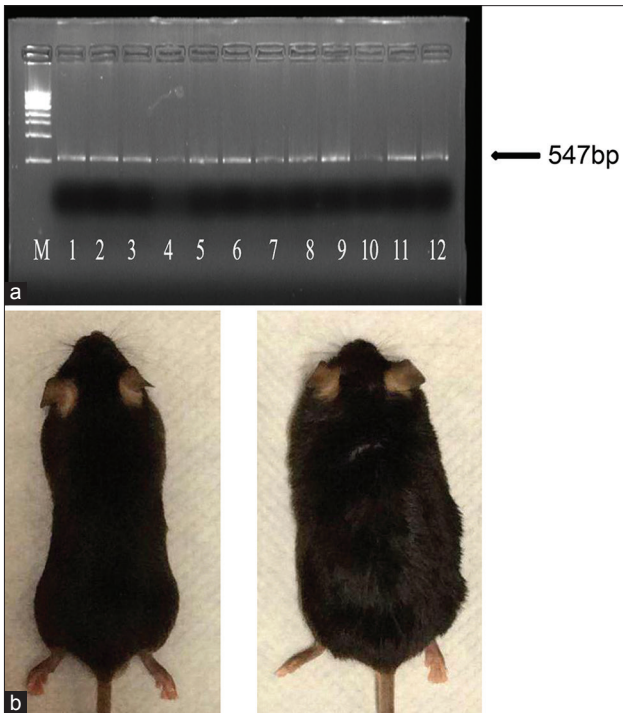
摘要

背景: 由NOD-样受体蛋白3 (NLRP3)、凋亡相关斑点样蛋白 (ASC) 和半胱氨酸天冬氨酸酶-1 (caspase-1) 组成的NLRP3炎症体参与了许多肾脏病的炎症反应, 且此炎症体能被嘌呤能2X7受体 (P2X7R) 激活。本研究拟探讨P2X7R是否参与了肥胖相关性肾小球病 (ORG) 的足细胞损伤, 且此作用是否通过NLRP3炎症体介导。

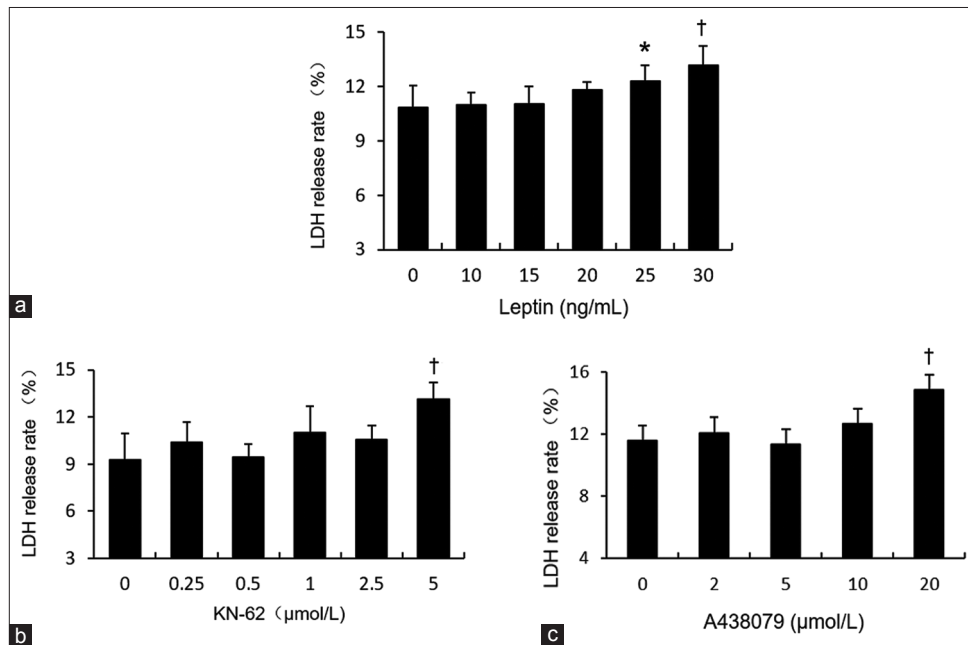
方法: 用高脂饲料喂养小鼠制作ORG模型进行整体体内研究, 并用瘦素刺激培养的条件性永生小鼠足细胞进行体外研究。P2X7R和NLRP3炎症体各组份 (NLRP3、ASC和caspase-1) 及足细胞相关分子 (nephrin、podocin和结蛋白) 的mRNA及蛋白质表达分别用实时半定量PCR及Western印迹法进行检测。

结果: ORG小鼠整体研究显示, 小鼠肾皮质中 (共聚焦显微镜检查显示实际在足细胞中) 的P2X7R和NLRP3炎症体各组份表达显著上调, NLRP3炎症体活化, 且伴随出现了小鼠足细胞损伤 (包括形态学表现及足细胞相关分子表达改变)。用瘦素刺激的足细胞体外研究, 也发现了与上相似的P2X7R和NLRP3炎症体表达上调/活化, 和足细胞相关分子表达的改变, 而上述所有变化均能被P2X7R拮抗剂KN-62或 A438079拮抗。

结论: P2X7R能激活NLRP3炎症体, ORG时足细胞中P2X7R和NLRP3炎症体的激活能参与足细胞损伤。



Supplementary Figure 1: (a) Identification of genetic background of mice by PCR. M: DNA marker, from bottom to top was 500 bp, 750 bp, 1000 bp, 2000 bp, 3000 bp, 4000 bp, and 5000 bp 1–12: Genome-amplified fragments from the randomly selective mice. (b) Photographs of mice at the 12th week. The mice in the control group were fed with a low-fat diet (left) and the mice in the obesity-related glomerulopathy model were fed with a high-fat diet (right).



Supplementary Figure 2: Determination of the concentrations of Leptin, KN-62, and A438079 in cell experiments by LDH release assay. Histograms (a-c) show the test results of leptin, KN-62, and A438079, respectively. Values are represented as mean \pm SD ($n = 6$). * $P < 0.05$, † $P < 0.01$, compared with control group. SD: Standard deviation.

Supplementary Table 1: Primer sequences for real-time quantitative RT-PCR analysis

Target	Primer sequence (5'-3')	Length (bp)
Nephrin		
Forward	GTCTGGGGACCCCTCTATGA	209
Reverse	CAGGTCTTCTCCAAGGCTGT	
Podocin		
Forward	CAGAAGGGGAAAAGGCTGCT	205
Reverse	GATGCTCCCTTGTGCTCTGT	
Desmin		
Forward	GTTTCAGACTTGACTCAGGCAG	106
Reverse	TCTCGCAGGTGTAGGACTGG	
P2X7R		
Forward	CACCGTGCTTACAGGTGCTA	115
Reverse	CGGTCTTGGGGAACCTCTTC	
NLRP3		
Forward	TCTGCACCCGGACTGTAAAC	131
Reverse	CATTGTTGCCCAGGTTCAGC	
ASC		
Forward	CTTGTCAGGGATGAACTCAAAA	154
Reverse	GCCATACGACTCCAGATAGTAGC	
Pro-caspase-1		
Forward	ACAAGGCACGGGACCTATG	237
Reverse	TCCCAGTCAGTCCTGGAAATG	
GAPDH		
Forward	TGTGAACGGATTTGGCCGTA	206
Reverse	GATGGGCTTCCCGTTGATGA	

PCR: Polymerase chain reaction; RT: Reverse transcription; ASC: Apoptosis-associated speck-like protein containing CARD; NLRP3: Nucleotide-binding and oligomerization domain-like receptor protein 3; P2X7R: Purinergic 2X7 receptor.

Supplementary Table 2: Primary and secondary antibodies for Western blot assay

Primary antibody	Dilution	Secondary antibody
Rabbit anti-nephrin pAb (Abcam, ab58968)	1:500	Goat anti-rabbit IgG secondary Antibody (LI-COR biosciences)
Rabbit anti-podocin pAb (Sigma- Aldrich, P0372)	1:500	Ditto
Rabbit anti-desmin pAb (Abcam, Ab15200)	1:500	Ditto
Rabbit anti-P2X7R pAb (Alomone Labs, APR-004)	1:500	Ditto
Rabbit anti-NLRP3 pAb (Novus Biologicals, NBP2-12446)	1:500	Ditto
Rabbit anti-ASC pAb (Santa Cruz Biotechnology, SC-22514R)	1:200	Ditto
Rabbit anti-caspase-1 P10 pAb (Santa Cruz Biotechnology, SC-514)	1:200	Ditto
Mouse anti- β -actin mAb (Sigma, A5316)	1:10000	Goat anti-mouse IgG secondary Antibody (LI-COR biosciences)

ASC: Apoptosis-associated speck-like protein containing CARD; NLRP3: Nucleotide-binding and oligomerization domain-like receptor protein 3; P2X7R: Purinergic 2X7 receptor.